Available online at www.sciencedirect.com
ScienceDirect
Journal of Solid State Chemistry 180 (2007) 812–817
JOURNAL OF SOLID STATE CHEMISTRY
www.elsevier.com/locate/jssc

Structural modulation in $K_2V_3O_8$

B.C. Chakoumakos[a,*], R. Custelcean[a], T. Kamiyama[b], K. Oikawa[c], B.C. Sales[a], M.D. Lumsden[a]

[a]Oak Ridge National Laboratory, Neutron Scattering Science Division, P.O. Box 2008, bldg 7962, Oak Ridge, TN 37831-6393, USA
[b]Institute of Materials Structure Science, High Energy Accelerator Research Organization, Tsukuba, Ibaraki 305-0801, Japan
[c]Quantum Beam Science Directorate, Japan Atomic Energy Agency, Tokai, Ibaraki 305-0801, Japan

Received 12 September 2006; received in revised form 22 November 2006; accepted 24 November 2006
Available online 9 December 2006

Abstract

To elucidate the phase transition at 115 K in the fresnoite-type compound $K_2V_3O_8$, we undertook temperature-dependent neutron powder diffraction and single-crystal X-ray diffraction (XRD). For structure refinements in the nominal space group *P*4*bm*, the most dramatic change is evidenced by the *a* cell edge, which initially expands on cooling, then abruptly begins to contract at 115 K. The *c* cell edge contracts monotonically. The atomic displacement parameters (ADPs) also deviate from their expected temperature dependence at 115 K, where the oxygen atoms in the vanadium oxide plane exhibit an increase in apparent positional disorder. Similar changes in lattice parameters and ADPs are observed from the single-crystal XRD refinements. Below 115 K, weak superlattice reflections are clearly evident in XRD patterns recorded by a CCD detector, and these extra reflections can be indexed with the wave vector $\pm 1/3\langle 110\rangle^* + 1/2c^*$. Possible space groups for the modulated structure are $P4_2bc$ and *P*4*nc*.

Keywords: $K_2V_3O_8$ fresnoite-type structure; Low-temperature phase transition; Low temperature average structure refinement; Crystal structure modulation; Nonlinear optical material

1. Introduction

$K_2V_3O_8$ has the fresnoite-type structure with the chemical formula $A_2B_3O_8$, where $A = K$, Rb, Cs, NH_4, H_3O, Sr, Ba; and $B =$ Si, Ti, V, Mn, Cu, Ge. The average parent *P*4*bm* crystal structure is composed of rigid corner-connected $V^{5+}O_4$ tetrahedra and $V^{4+}O_5$ square pyramids in sheets alternating with layers of *A* cations (Fig. 1) [1]. The vanadate fresnoites are antiferromagnets, where the VO_5 square pyramids contain the magnetic V^{4+} ions with $S = 1/2$, whereas the tetrahedra contain nonmagnetic V^{5+} ions [2]. The $A_2V_3O_8$ fresnoites in particular have attracted attention due to their novel low-temperature magnetic properties [3–5] and their nonlinear optical properties [6]. Theoretical studies suggest that the crystallographic symmetry and magnetic ordering in these systems should allow the simultaneous occurrence of chiral inhomogeneous magnetic structures and weak ferromagnetism [7] and new types of incommensurate magnetic structures are possible, e.g., chiral helices with rotation of staggered magnetization and oscillations of the total magnetization [8,9]. Fresnoite-type structures in general are of interest because of their susceptibility to displacive structural phase transitions [10–19].

At 110 K infrared, permittivity, and heat capacity measurements [20] indicate a structural transition occurs in $K_2V_3O_8$, which is suggested to be marked by a small distortion of the coordination geometry of the magnetic V^{4+} ion. Here we report X-ray single-crystal and neutron powder diffraction studies, which further elucidate the low temperature structural modulation in $K_2V_3O_8$.

2. Experimental methods

2.1. Synthesis

Single crystals of $K_2V_3O_8$ (typical dimensions $0.5 \times 0.5 \times 0.05\,cm^3$) were grown in a platinum crucible

*Corresponding author. Fax: +1 865 574 6268.
E-mail address: chakoumakobc@ornl.gov (B.C. Chakoumakos).

0022-4596/$ - see front matter © 2006 Elsevier Inc. All rights reserved.
doi:10.1016/j.jssc.2006.11.033

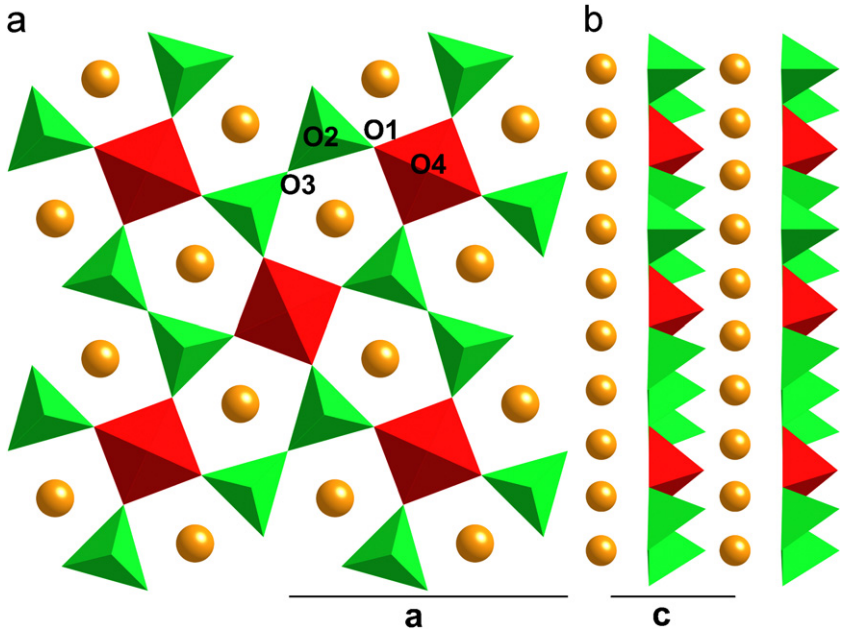

Fig. 1. The $K_2V_3O_8$ fresnoite-type crystal structure (ideally *P4bm*), with the $V^{5+}O_4$ tetrahedra shaded green and $V^{4+}O_5$ square pyramids shaded red. The spheres represent the K atoms: (a) [001] projection, and (b) [110] projection.

by cooling VO_2 in a molten KVO_3 flux sealed inside a silica ampoule.

2.2. Neutron powder diffraction

Single-crystals were powdered. Neutron powder diffraction data were measured at each temperature (5, 10, 15, 20, 30, 40, 70, 100, 110, 130, 170, 200, 230, 270, and 295 K) for ~3 h on the time-of-flight neutron diffractometer Vega [21] at the pulsed spallation neutron facility KENS. The sample was contained in cylindrical vanadium cell 9.2 mm in diameter, 20 mm in height, with wall thickness 0.150 mm. The Rietveld refinements from the neutron data used RIETAN-2001T [22]. The neutron scattering lengths used were taken from Sears [23], K (3.67 fm), V (−0.3824 fm), and O (5.803 fm). Owing to the small scattering length of V, the V atom positions and their displacement parameters were fixed at values corresponding to those from the X-ray refinement results or their low temperature extrapolation.

2.3. Single-crystal X-ray diffraction (XRD)

A suitably sized crystal was cleaved from a large crystal and mounted on a Bruker PLATFORM three-circle X-ray diffractometer operated at 50 keV and 40 mA, equipped with a 4K APEX CCD detector and a crystal-to-detector distance of ~4.7 cm. An Oxford Cryostream open flow nitrogen cooler was used to cool the crystal. A sphere of three-dimensional (3D) data was collected for each temperature of 240, 200, 120, 100 and 80 K using graphite-monochromatized Mo$K\alpha$ X-radiation and frame widths of 0.3° in ω and 10 s counting time per frame. Details of the data acquisition and refinement parameters are given in Table 1. The data were analyzed to locate peaks for the determination of the unit-cell parameters. All reflections were indexed based on a tetragonal unit cell. The intensity data were reduced and corrected for Lorentz, polarization, and background effects using the program

Table 1
Crystal data, data collection and refinement results for $K_2V_3O_8$

Crystal data	
$K_2V_3O_8$	Mo$K\alpha$ radiation
$M_r = 359.02$	Cell parameters from 4245 reflections
Tetragonal, *P4bm*	$\Theta = 2.5$–$28.3°$
$a = 8.8954(1)$ Å	$\mu = 4.32\,mm^{-1}$
$c = 5.2472(1)$ Å	$T = 293$ K
$V = 415.20(2)$ Å^3	Green plate
$Z = 2$	$0.27 \times 0.18 \times 0.09$ mm
$D_x = 2.872\,mg\,m^{-3}$	
Data collection	
Bruker Smart Apex CCD	552 reflections with $I > 4\sigma(I)$
Diffractometer	$R_{int} = 0.026$
ω scans	$\theta_{max} = 28.3$
Absorption correction: multi-scan [23]	$h = -11 \rightarrow 11$
$T_{min} = 0.387$, $T_{max} = 0.696$	$k = -11 \rightarrow 11$
4245 measured reflections	$l = -6 \rightarrow 7$
553 independent reflections	
Refinement	
Refinement on F^2	$(\Delta/\sigma)_{max} = 0.001$
$R[F^2 > 4\sigma(F^2)] = 0.016$	$\Delta\rho_{max} = 0.37\,eÅ^{-3}$
$wR(F^2) = 0.034$	$\Delta\rho_{min} = -0.21\,eÅ^{-3}$
$S = 1.15$	Extinction correction: SHELXL97
553 reflections	Extinction coefficient: 0.0537(4)
39 parameters	Absolute structure: Flack [25]
$w = 1/[\sigma^2 (F_o^2) + (0.0194P)^2 + 0.0734P]$, where $P = (F_o^2 + 2F_c^2)/3$	Friedel pairs not merged
	Flack parameter: 0.09(3)

SAINT [24], and the unit-cell dimensions were refined using least-squares methods. The systematic absences of reflections were consistent with the space group *P4bm*, and the Flack parameter of $\leqslant 0.09(3)$ for each temperature confirms that the absolute structure was correctly determined [25]. An empirical correction for X-ray absorption was made using the program SADABS [26].

The initial structure model for the crystal was taken from the neutron diffraction results. Scattering curves for neutral atoms, together with anomalous dispersion corrections, were taken from the *International Tables for* X-ray *Crystallography, Vol. C* [27]. The SHELXTL Version 5 [28] series of programs was used for the solution and refinement of the crystal structures. The refined room temperature structural parameters from the single-crystal X-ray diffraction data are given in Table 2, and the Crystallographic Information Files for all temperatures of the X-ray diffraction data are deposited.

3. Results and discussion

The onset of the structural modulation is evident in the variation of the *a*-lattice parameter of the average structure as a function of temperature (Fig. 2). Upon cooling from room temperature, initially the *a*-lattice parameter expands and the *c*-lattice parameter contracts. At 115 K the *a*-lattice parameter begins to contract. The quality of the Rietveld refinements of the neutron powder diffraction data using the average structure progressively worsens as the temperature is decreased below 115 K, which is a strong indicator that the average structure model no longer adequately describes the crystal structure. In addition, the temperature dependence of some of the atomic displacement parameters (ADPs) exhibits anomalous behavior below 115 K (Fig. 3). In particular, the displacements of O1 (bridging pyramid and tetrahedron) and O3 (bridging tetrahedra) begin to increase below 115 K, whereas the displacements of O2 (apical to tetrahedron) and O4 (apical to pyramid) exhibit monotonic decreases. Overall, the displacement of the O4 atom is larger by a constant amount at all temperatures than those of the other oxygen atoms, which suggests that O4 is positionally disordered by about 0.07 Å as compared to the other oxygen atoms independent of the structural modulation. We also expect the displacement of the K atom to be more similar to the V atom because of their similar masses, however the K atom displays the largest displacement at the higher temperatures. This again suggests that the K atom manifests some positional disorder independent of the structural modulation. From the X-ray results, the temperature dependence of the V^{5+} and V^{4+} displacements appear to flatten below the 115 K phase transition. The ADPs determined from the X-ray and neutron diffraction experiments are essentially the same, except for the steeper slope of that of the K atom from the latter. Overall, the analysis of the temperature dependence of the ADPs identifies O1, O3, and the vanadium atoms as principal players in the structural modulation.

By examining the anisotropic displacement parameters (Fig. 4), we can further identify which eigenvectors exhibit anomalous temperature dependence. The eigenvectors of the apical oxygen atoms O2 and O4 and the K atoms are well behaved. Both O2 and O4 are somewhat anisotropic with their principal displacement being within the vanadium oxide layer. The K atom is distinctly anisotropic with the principal displacement close to the $\langle 110 \rangle$ directions. Both of the bridging oxygen atoms (O1 and O2) are somewhat anisotropic. The u_2 eigenvector of the O1 atom

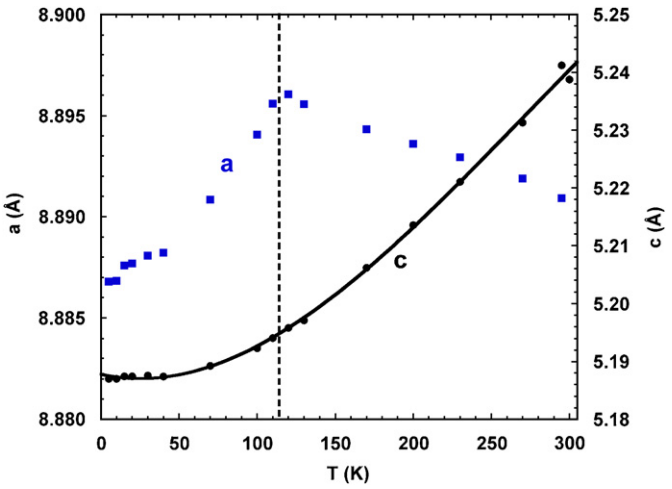

Fig. 2. Temperature dependence of the lattice parameters from neutron powder diffraction data. The 115 K onset of the structural modulation is indicated by the dashed line.

Table 2
Room temperature structural parameters for $K_2V_3O_8$ from least-squares refinement of single-crystal X-ray diffraction data

Atom	Site	Symmetry	*x*	*y*	*z*	U_{eq}
K	4*c*	..*m*	0.66907(4)	0.16907(4)	0.1723(1)	0.0327(1)
V^{5+}	4*c*	..*m*	0.36608(2)	0.13392(2)	0.64187(7)	0.0116(1)
V^{4+}	2*a*	4..	0	0	0.63650(8)	0.0124(1)
O1	8*d*	1	0.1921(1)	0.0866(1)	0.5282(2)	0.0219(2)
O2	4*c*	..*m*	0.3698(1)	0.1301(1)	0.9530(3)	0.0235(4)
O3	2*b*	2.*mm*	0	1/2	0.5173(3)	0.0186(5)
O4	2*a*	4..	0	0	0.9410(5)	0.0308(5)

Note: Space group *P4bm*, $a = 8.8954(1)$ Å, $c = 5.2472(1)$ Å.

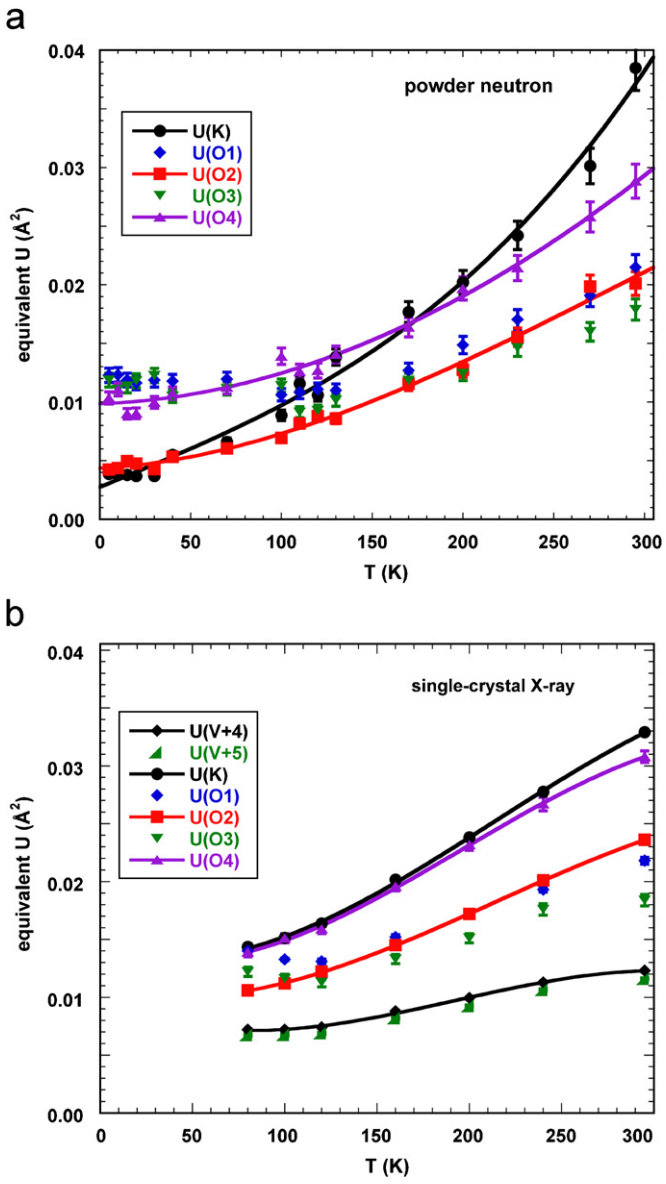

Fig. 3. Temperature dependence of the equivalent isotropic displacement parameters from refinements of (a) neutron powder diffraction and (b) X-ray single-crystal diffraction data.

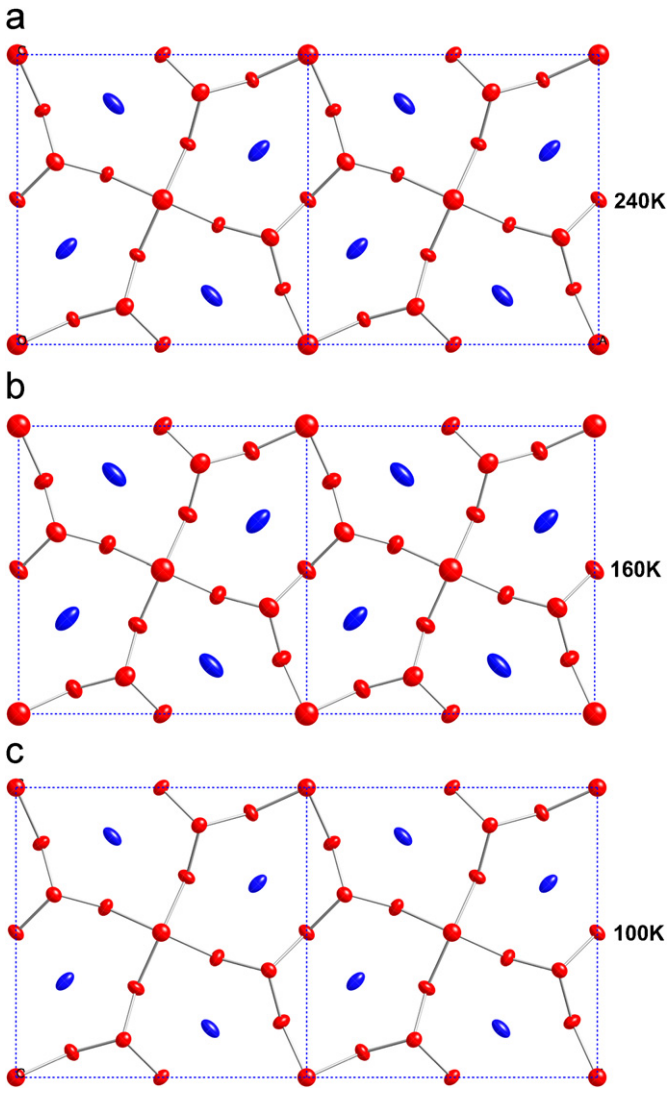

Fig. 4. Anisotropic displacement ellipsoids (99.9% probability) for $K_2V_3O_8$ for three temperatures, 240, 160, and 100 K, from refinement of single-crystal X-ray diffraction data using the average *P*4*bm* structure model. Oxygen atoms are red, and the potassium atoms are blue. The bond connectivity is shown by the "sticks." Two unit cells are outlined and the [001] projection corresponds to that in Fig. 1(a), so that the atom labeling can be easily deduced.

(bridging pyramid and tetrahedron) shows anomalous temperature dependence below 115 K, and is directed roughly perpendicular to [001] and to bonds between the O2 atom and the neighboring vanadium atoms. The u_1 eigenvector of the O3 atom is anomalous below 115 K, and is directed parallel to [110]. Both vanadium atoms have uniaxial displacement ellipsoids with the largest displacement along [001]. The smaller in-plane displacements have anomalous temperature dependences below 115 K. Given that all of the anomalous eigenvectors lie within the vanadium oxide layer and involve the vanadium and bridging oxygen atoms (O1 and O3), suggests that the structural distortion at 115 K is accomplished by in-plane rotation about the *c*-axis of the vanadium oxide tetrahedron and pyramid. The V–O bond length changes with temperature are consistent with this picture. As might be expected, all of the K–O bonds contract slightly, which is the mechanism by which the *c*-axis contracts.

Below 115 K weak superlattice reflections are clearly evident in X-ray diffraction patterns recorded by the CCD detector, and these extra reflections can be indexed with the wave vector $\pm 1/3\langle 110\rangle^* + 1/2c^*$, where the $\langle 110\rangle^*$ and c^* directions refer to the parent unit cell. Table 3 compares modulation wave vectors observed for this and other fresnoite-type compounds. The refined lattice parameters for this $3\times3\times2$ supercell are $a = 26.688(3)$ Å and $c = 10.383(2)$ Å. To explore for the possible space groups for the superstructure, PowderCell [29] was used. First the $3\times3\times2$ supercell with the parent *P*4*bm* symmetry was generated. Then maximal subgroups were enumerated that

Table 3
Modulation wave vectors observed in some fresnoite-type compounds

Composition	Modulation wave vectors	T_c (K)	Over (under)-bonding of *A*-site (%)	Reference
$Sr_2TiOSi_2O_7$	$\sim\pm0.3\langle110\rangle_p^*$ $\sim\pm0.3\langle110\rangle_p^*+1/2c^*_p$	>293	−18.9	Höche et al. [18]
$Ba_2TiOGe_2O_7$	$\sim\pm0.3\langle110\rangle_p^*+1/2c^*_p$	1123	−15, −9.2	Höche et al. [17]
$Ba_2TiOSi_2O_7$	$\sim\pm0.3\langle110\rangle_p^*+1/2c^*_p$	433	−1.6	Withers et al. [12] and Bindi et al. [13]
$Ba_2VOSi_2O_7$	$\sim\pm0.3\langle110\rangle_p^*+1/2c^*_p$	>293	−8.3	Höche et al. [11]
$K_2VOV_2O_7$	$\pm1/3\langle110\rangle_p^*+1/2c^*_p$	115	+3.2	This work
$Rb_2VOV_2O_7$	$\sim0.16c^*$	269	+9.4	Withers et al. [10]

were consistent with the $3\times3\times2$ cell. These included *P*4*bm*, $P4_2bc$, *P*4*nc*, and $P4_2nm$. The 80 K single-crystal X-ray data were used to test these possible space groups by trying least-squares refinement using SHELX97 [28]. The *R*1 agreement factors from the refinement results of the observed data including the supercell reflections were 0.160, 0.082, 0.081, and 0.161, respectively, using isotropic ADPs. This suggests that $P4_2bc$ and *P*4*nc* are plausible space groups for the modulated structure below 115 K.

Some discussion has been given regarding the relationship between the degree of overbonding of the interlayer cation and the amplitude of the observed modulation in the fresnoite compounds [10]. Generally, divalent interlayer cations are overbonded and the greater the extent of overbonding, the larger the modulation amplitude. However, for monovalent interlayer cations, the bond valence sum is underbonding (Table 3). The modulation observed in $Rb_2V_3O_8$ is unlike that in $K_2V_3O_8$ and the other fresnoite compounds, for which the modulations have been studied in detail (Table 3). The modulation we deduce here for $K_2V_3O_8$ is similar to that observed in $Sr_2TiOSi_2O_7$, $Ba_2TiOGe_2O_7$, $Ba_2TiOSi_2O_7$, and $Ba_2VOSi_2O_7$, except that it appears to be commensurate. Further details can be achieved by electron diffraction study at low temperatures.

The structural phase transition at 115 K in $K_2V_3O_8$ is the onset of a $3\times3\times2$ superlattice modulation associated with rotations of the vanadium oxide polyhedra about the *c*-axis, and is likely driven by the collapse of the vanadate layers about the interlayer potassium atom as the structure thermally contracts. Analysis of the temperature dependence of the ADPs gives a picture of the structural distortion at the phase transition. The thermal contraction of $K_2V_3O_8$ is quite anisotropic, the *c*-axis contracts by 1% compared to the *a*-axis by 0.05% between 300 and 5 K. Initially the *a*–*b* plane expands slightly until the 115 K transition is reached.

Acknowledgments

We thank Cara Nygren for collecting the room temperature, single-crystal, X-ray diffraction data. This research was sponsored by the Division of Materials Sciences and Engineering, Office of Basic Energy Sciences, US Department of Energy, under contract DE-AC05-00OR22725 with Oak Ridge National Laboratory, managed and operated by UT-Battelle, LLC.

Appendix A. Supplementary materials

Supplementary data associated with this article can be found in the online version at: doi:10.1016/j.jssc.2006.11.033.

References

[1] J. Galy, A. Carpy, Acta Crystallogr. B 31 (1975) 1794–1795.
[2] G. Liu, J.E. Greedan, J. Solid State Chem. 114 (1995) 499–505.
[3] M.D. Lumsden, B.C. Sales, D. Mandrus, S.E. Nagler, J.R. Thompson, Phys. Rev. Lett. 86 (2001) 159–162.
[4] B.C. Sales, M.D. Lumsden, S.E. Nagler, D. Mandrus, J. Jin, Phys. Rev. Lett. 88 (2002) 095901.
[5] R.C. Rai, J. Cao, J.L. Musfeldt, D.J. Singh, X. Wei, R. Jin, Z.X. Zhou, B.C. Sales, D. Mandrus, Phys. Rev. B 73 (2006) 075112.
[6] J.K. Yuan, P.Z. Fu, J.X. Wang, F. Guo, Z.P. Yang, Y.C. Wu, Prog. Cryst. Growth Character. Mater. 40 (2000) 103–106.
[7] A.N. Bogdanov, U.K. Rossler, M. Wolf, K.H. Muller, Phys. Rev. B 66 (2002) 214410.
[8] A.N. Bogdanov, U.K. Rossler, M. Wolf, K.H. Muller, J. Magn. Magn. Mater. 272–276 (Part 1) (2004) 332–334.
[9] A.L. Chernyshev, Phys. Rev. B 72 (2005) 174414.
[10] R.L. Withers, T. Höche, Y. Liu, S. Esmaeilzadeh, R. Keding, B.C. Sales, J. Solid State Chem. 177 (2004) 3316–3323.
[11] T. Höche, S. Esmaeilzadeh, R.L. Withers, H. Schirmer, Z. Kristallogr. 218 (2003) 788–794.
[12] R.L. Withers, Y. Tabira, Y. Liu, T.A. Höche, Phys. Chem. Miner. 29 (2002) 624–632.
[13] L. Bindi, M. Dusek, V. Petricek, P. Bonazzi, Acta Crystallogr. B 62 (2006) 1031–1037.
[14] P.A. van Aken, T. Höche, F. Heyroth, R. Keding, R. Uecker, Phys. Chem. Miner. 31 (2004) 543–552.
[15] T. Höche, P.A. van Aken, M. Grodzicki, F. Heyroth, R. Keding, R. Uecker, Philos. Mag. 84 (2004) 3117–3132.
[16] T. Höche, W. Neumann, Ultramicroscopy 96 (2003) 181–190.
[17] T. Höche, S. Esmaeilzadeh, R. Uecker, S. Lidin, W. Neumann, Acta Crystallogr. B: Struct. Crystallogr. Cryst. Chem. 59 (2003) 209–216.
[18] T. Höche, W. Neumann, S. Esmaeilzadeh, R. Uecker, M. Lentzen, C. Russel, J. Solid State Chem. 166 (2002) 15–23.
[19] T. Höche, W. Neumann, Ferroelectrics 250 (2001) 67–70.
[20] J. Choi, Z.T. Zhu, J.L. Musfeldt, G. Ragghianti, D. Mandrus, B.C. Sales, J.R. Thompson, Phys. Rev. B 65 (2002) 054101.
[21] T. Kamiyama, S. Torii, K. Mori, K. Oikawa, S. Itoh, M. Furusaka, S. Satoh, T. Egami, F. Izumi, H. Asano, Mater. Sci. Forum 321–324 (2000) 302–307.
[22] F. Izumi, T. Ikeda, Mater. Sci. Forum 321–324 (2000) 198–203.
[23] V.F. Sears, Neutron News 3 (1992) 26–37.

[24] SHELXTL 6.12, Bruker AXS, Inc., Madison, WI, 1997.
[25] H.D. Flack, Acta Crystallogr. A 39 (1983) 876–881.
[26] G.M. Sheldrick, SADABS, Program for Empirical Absorption Correction of Area Detector Data, Institüt fur Anorganische Chemie der Universität, Tammanstrasse 4, D-3400 Göttingen, Germany, 1996.
[27] A.J.C. Wilson (Ed.), International Tables for X-ray Crystallography, vol. C, Kluwer Academic, London, 1992.
[28] G.M. Sheldrick, SHELX97, Programs for Crystal Structure Analysis. Release 97-2, Institüt fur Anorganische Chemie der Universität, Tammanstrasse 4, D-3400 Göttingen, Germany, 1997.
[29] W. Kraus, G. Nolze, PowderCell 1 (1996) 8.